# Analysis of Sea Level Changes in Eastern Taiwan Coast—Case of Yilan Area

Hui-Ming Fang, Po-Han Chang, and Hsing-Yu Wang*

***Abstract*—This study considers the impact of extreme climates on most of the world's land and seas, which may cause the average sea level to rise due to global climate change. Affected by the rise of sea level, it will change the distribution characteristics of sea tides, waves and currents. When the distribution of tides, waves and currents in the sea area changes, it may cause changes in the overall environmental characteristics of the estuary and coastal areas, and further affects the function of coastal protection facilities. This study takes the sea area of Yilan as an example, and analyzes the problem of sea level rise in the three-in-one climate change (including sea level rise, typhoon and heavy rain). For the analysis of sea level rise, this study calculates tide level data in three ways, the first is simple moving average (SMA), then there are empirical mode decomposition (EMD) and ensemble empirical mode decomposition (EEMD) in the hilbert-huang transform (HHT) for sea level rise analysis. The use of ensemble empirical mode decomposition (EEMD) is because when modal confusion occurs in empirical mode decomposition (EMD), the occurrence of modal confusion can be reduced by adding the decomposed signal to the white noise sequence. Comparing the analysis results of the three respectively, the result obtained by using simple moving average (SMA) is the smallest (2.78 mm/yr), and the result obtained by using ensemble empirical mode decomposition (EEMD) calculation is the largest (4.11mm/yr). By analyzing the results obtained, it can be provided for assessing future hydrological and environmental changes based on climate change conditions.**

***Index Terms*—Climate change, sea level rise, simple moving average (SMA), empirical mode decomposition (EMD), ensemble empirical mode decomposition (EEMD)**

## I. Introduction

In recent years, the issue of climate change arising from the impact of global warming, especially sea level rise, is closely related to other environmental change issues. Among them are discussions on sea level rise, such as [1–5]. The results show that the global sea level rise rate in the twentieth century is about 1.5–2.4 mm/yr. Church *et al*. [4] analyzed the sea level data of the Permanent Service for Mean Sea Level (PSMSL) from 1880 to 2009, and found that the global sea level rose on average by about 210 mm. Among them, between 1900 and 2009, the average rate of global sea level rise was 1.7 ±0.2 mm/yr. In addition, based on the analysis of satellite data from 1993 to 2009, the average rate of global sea level rise was 3.2 ±0.4 mm/yr. According to the Intergovernmental Panel on Climate Change (IPCC) AR6 report in 2021 [6], the records of extreme climate and climate events observed since 1950 show that the probability of occurrence of frequency and duration of warm periods, rainfall and intensity, severe tropical cyclone activity, and extreme high sea level caused by climate change has increased. The report mentioned that from 1901 to 2018, the average global sea level rose by 200 mm; the average global sea level rise rate was 1.3 mm/yr from 1901 to 1971, and 1.9 mm/yr from 1971 to 2006. However, the average rate of sea level rise between 2006 and 2018 increased to 3.7 mm/yr. The overall study results show an increasing trend in the rate of sea level rise.

Extreme climates have a great impact on most of the world's land and sea areas, such as changes in hydrological conditions, which will directly affect the environmental characteristics of estuaries and coasts, as well as the function of coastal protection facilities. For studies on sea level rise around Taiwan, for example, Merrifield [7] used satellite data from 1993 to 2009 to analyze sea level changes in the Pacific Ocean. The results show that the rate of sea level rise in the southwest Pacific is higher than that of the rest of the Pacific Ocean, while the average rate of sea level rise in the seas around Taiwan is about 4.5-7 mm/yr. Doong *et al*. [8] analyzed the East Asian tide station data from PSMSL and showed that the mean sea level rise rate along the East Asian coast was 2.77 mm/yr. Among them, the average sea level rise rate of Keelung at the northern of Taiwan was 5.91 mm/yr from 1980 to 2001, and that of Kaohsiung at the southern was 3.64 mm/yr from 1975 to 2008. Kuo *et al*. [9] used multivariate fitting of satellite altimetry data to estimate that the sea level rise rate near Taiwan caused by climate factors is about 2 mm/yr. Then, using the analysis results, it is estimated that in 2050, the sea level around Taiwan will rise by about 90 mm relative to 2012.

Since Taiwan is located in a typhoon-prone area in the western Pacific, according to the statistics of typhoon data from 1911 to 2020 by the Central Weather Bureau of Taiwan, the proportion of typhoons that landed from the east of Taiwan accounted for about 73.4%, of which Yilan in the east accounted for the largest proportion of 21.8%. This study refers to the Key Findings in Climate Science from IPCC AR6 Report published by the Taiwan Climate Change Projection Information and Adaptation Knowledge Platform on March 1, 2022 [10]. The content of the report pointed out that under the scenario of IPCC AR6 warming by 4 ℃, the rainfall intensity, flooding area, typhoon storm surge, and the impact range of sea level rise and flooding in Yilan tended to increase. Considering that the rise of sea level caused by the impact of global warming may change the distribution characteristics of tides, waves and currents in the sea area, and then affect the problems related to coastal preservation.

Manuscript received May 27, 2022; revised July 2, 2022; accepted August 3, 2022.

H. M. Fang and P. H. Chang are with the Department of Harbor and River Engineering, National Taiwan Ocean University, Keelung, Taiwan.

H. Y. Wang is with the Department of Shipping Technology, National Kaohsiung University of Science and Technology, Kaohsiung, Taiwan.

*Correspondence: hywang05@nkust.edu.tw (H.Y.W.)

doi: 10.18178/ijesd.2023.14.4.1442

Therefore, this study aims at the sea level rise problem of the three-in-one climate change (sea level rise, typhoon and heavy rain), and uses Moving Average (MA), and Empirical Mode Decomposition (EMD) and Ensemble Empirical Mode Decomposition (EEMD) of Hilbert-Huang Transform (HHT), respectively, to analyze the change trend of the average sea level in the Yilan areas of Taiwan.

## II. Environment Background and Harmonic Analysis

This study collects water level data in the Yilan sea area and analyzes sea level changes under climate change. Referring to the information of the two tidal stations set up by the Central Weather Bureau of Taiwan in Yilan, the positions of the tidal stations are shown in Fig. 1, which are located in the Wu-Shi Harbor and Su'ao Port. Among the two stations, the tidal station in Su'ao Port has the longest data year. The station was set up on January 1, 1981 and began to observe until now. Therefore, this study collects the tidal station data of Su'ao Port, and the data length is from January 2004 to September 2021 for analysis.

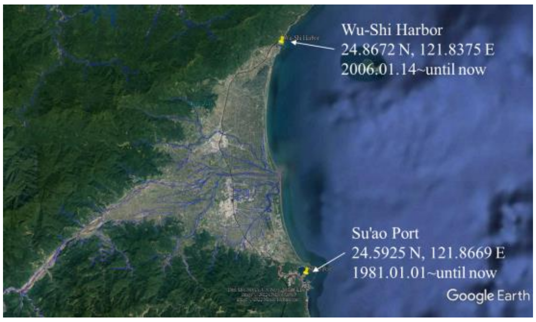


Fig. 1. Tidal station information in Yilan.
*Source: Central Weather Bureau of Taiwan; Google Earth*

However, in the process of recording data, the instruments of the Taiwan tidal station may change their positions due to human factors such as maintenance, or be affected by natural disasters such as typhoons, resulting in instrument damage or stop recording. The above reasons for the damage of the instrument or the stop of recording will affect the actual recorded tide level data. The actual measured data of the Su'ao tide level station is shown in Table I. Between 2004 and 2021, the record level of the data is probably more than 80%. Although there are more than 80% of the recorded data, in order to provide the observed water level data for subsequent applications, harmonic analysis is used to supplement the water level data.

TABLE I: Completeness of Measured Tide Level Data at Su'ao Tidal Station

| Year; Collection rate | Year; Collection rate | Year; Collection rate |
|---|---|---|
| 2004; 87.37% | 2005; 97.64% | 2006; 98.38% |
| 2007; 98.96% | 2008; 96.72% | 2009; 97.96% |
| 2010; 98.79% | 2011; 98.26% | 2012; 93.60% |
| 2013; 93.64% | 2014; 91.75% | 2015; 85.83% |
| 2016; 95.08% | 2017; 94.33% | 2018; 82.84% |
| 2019; 94.79% | 2020; 90.14% | 2021; 99.47% |

Harmonic analysis is a more accurate analysis method for inferring tidal characteristics at present. Mainly, the tide is regarded as the sum of each sub-tidal, and the frequency, amplitude and retardation angle of each sub-tidal are deduced from the measured tidal data, and then the tidal shape and the future tidal data are predicted. Since the harmonic analysis only considers astronomical tides, factors such as storm tides and seafloor topography are not taken into account. In theory, there should be an infinite number of tidal divisions, but in practice, only the main 60 tidal divisions are used as the basis for analysis. The following function is the tidal division curve at any time:

$$y(t) = f \cdot H \cdot \cos\left(\omega t + \left(V_0 + u\right) - k\right) \tag{1}$$

where $y(t)$ is the tidal height of the partial tide, $f$ is the correction coefficient, $H$ is the amplitude of the partial tide, $\omega$ is the angular velocity of the partial tide, $\left(V_0 + u\right)$ is the balance argument, $k$ is the phase lag. When each tidal division is established, assuming that the tidal level change at any location is composed of the linear superposition of each tidal division, it can be expressed by harmonic analysis, as shown in Eq. (2):

$$Y(t) = H_0 + \sum_{i=1}^{N} y_i(t) = H_0 + \sum_{i=1}^{M} f_i \cdot H_i \cdot \cos\left(\omega_i t + \left(V_0 + u\right)_i - k_i\right) \tag{2}$$

where $Y(t)$ is the water level, $H_0$ is the average sea level, and $M$ is the number of tidal divisions. Eq. (2) can be replaced by trigonometric functions into Eq. (3):

$$\mathrm{Y}(t) = a_0 + \sum_{i=1}^{M}\left(a_i \cos \omega_i t + b_i \sin \omega_i t\right) \tag{3}$$

where $a_0 = H_0$, $a_i = f_i \cdot H_i \cdot \cos\left\lfloor \left(V_0 + u\right)_i - k_i \right\rfloor$, $b_i = f_i \cdot H_i \cdot \sin\left\lfloor \left(V_0 + u\right)_i - k_i \right\rfloor$.

However, most tidal data are recorded at time intervals of 6 minutes, not every minute and every second. Assuming that every interval $\Delta t$ will record a piece of data, if the data of time length $(2N+1)\Delta t$ is taken, and the midpoint of this time length is set as the start time, the entire period is:

$$t = n \cdot \Delta t,\ n = -N, -(N-1), ..., 0, 1, ..., N-1, N \tag{4}$$

and the tide level at the n[th] record moment is:

$$Y(n \cdot \Delta t) = a_0 + \sum_{i=1}^{M}\left[a_i \cos(\omega_i \cdot n \cdot \Delta t) + b_i \sin(\omega_i \cdot n \cdot \Delta t)\right] \tag{5}$$

Next, let the actual recorded tide level data be $\eta(n \cdot \Delta t)$, and the sum of squares of errors between the actual tide level and the estimated tide level is shown in Eq. (6):

$$\varepsilon = \sum_{n=-N}^{N}\left[Y(n \cdot \Delta t) - \eta(n \cdot \Delta t)\right]^2 \tag{6}$$

In order to minimize the error $\varepsilon$, the least squares method is used to differentiate the coefficients of Eq. (6) and make them zero, such as in Eqs. (7)–(9):

$$\frac{\partial \varepsilon}{\partial a_0} = \sum_{n=-N}^{N} \left[ Y(n \cdot \Delta t) - \eta(n \cdot \Delta t) \right] \frac{\partial Y}{\partial a_0} = 0 \quad (7)$$

$$\frac{\partial \varepsilon}{\partial a_i} = \sum_{n=-N}^{N} \left[ Y(n \cdot \Delta t) - \eta(n \cdot \Delta t) \right] \frac{\partial Y}{\partial a_i} = 0 \quad (8)$$

$$\frac{\partial \varepsilon}{\partial b_i} = \sum_{n=-N}^{N} \left[ Y(n \cdot \Delta t) - \eta(n \cdot \Delta t) \right] \frac{\partial Y}{\partial b_i} = 0 \quad (9)$$

In Eqs. (7)–(9), there are 2$N$+1 unknowns and 2$N$+1 equations. From this, the unknowns $a_0$, $a_i$ and $b_i$ can be obtained. Then use trigonometric functions to replace them into Eqs. (10)–(12):

$$a_0 - \sum_{i=1}^{M} \left( \frac{\sin\left[2N+1\right] \cdot \omega_i \cdot \frac{\Delta t}{2}}{(2N+1) \cdot \sin\left(\omega_i \cdot \frac{\Delta t}{2}\right)} \cdot a_i \right) = \frac{1}{2N+1} \sum_{n=-N}^{N} \eta(n \cdot \Delta t) \quad (10)$$

$$\sum_{i=1}^{M} a_i \cdot \frac{1}{2N+1} \left( \frac{\sin\left[(2N+1) \cdot (\omega_i - \omega_j) \cdot \frac{\Delta t}{2}\right]}{\sin\left[(\omega_i - \omega_j) \cdot \frac{\Delta t}{2}\right]} + \frac{\sin\left[(2N+1) \cdot (\omega_i + \omega_j) \cdot \frac{\Delta t}{2}\right]}{\sin\left[(\omega_i + \omega_j) \cdot \frac{\Delta t}{2}\right]} \right) = \frac{2}{2N+1} \sum_{n=-N}^{N} \left[ \eta(n \cdot \Delta t) \cdot \cos(\omega_j \cdot n \cdot \Delta t) \right] \quad (11)$$

$$\sum_{i=1}^{M} b_i \cdot \frac{1}{2N+1} \left( \frac{\sin\left[(2N+1) \cdot (\omega_i - \omega_j) \cdot \frac{\Delta t}{2}\right]}{\sin\left[(\omega_i - \omega_j) \cdot \frac{\Delta t}{2}\right]} + \frac{\sin\left[(2N+1) \cdot (\omega_i + \omega_j) \cdot \frac{\Delta t}{2}\right]}{\sin\left[(\omega_i + \omega_j) \cdot \frac{\Delta t}{2}\right]} \right) = \sum_{n=-N}^{N} \left[ \eta(n \cdot \Delta t) \cdot \sin(\omega_j \cdot n \cdot \Delta t) \right] \quad (12)$$

where $j = 1, 2, \ldots, M$. The coefficients of $a_0$, $a_1$ ... $a_M$, and $b_0$, $b_1$ ... $b_M$ can be obtained from the simultaneous equations of Eq. (10) to (12). The harmonic constant of the tide is:

$$H_0 = a_0; \quad H_i = \frac{1}{f_i} \sqrt{a_i^2 + b_i^2}; \quad k_i = (V_0 + u)_i + \tan^{-1} \frac{b_i}{a_i} \quad (13)$$

After using the harmonic analysis to complete the calculation of the missing parts of the original data, the long-term and continuous water level data can be provided to the HHT calculation, and the sea surface changes can be analyzed.

## III. Analysis of the Sea Level Rise

### A. Moving Average

According to different calculation methods, moving average can be divided into three methods: simple moving average (SMA), weighted moving average (WMA), and exponential moving average (EMA). Where Weighted Moving Average and Exponential Moving Average are based on Simple Moving Average. Data in different periods are added with different weights. The closer the data is, the greater the weight, which means the greater the impact on the average. However, the most commonly used method is the Simple Moving Average method currently used in various technical indicators and technical analysis. The calculation formula of Simple Moving Average method is Eq. (14):

$$F_{t+1} = \frac{D_t + D_{t-1} + D_{t-2} + \ldots + D_{t-n+1}}{n} \quad (14)$$

where $F_{t+1}$ is the forecast value of the next period, $n$ is the number of moving average periods, and $D_t$, $D_{t-1}$, $D_{t-2}$, $D_{t-n+1}$ are the data of the previous period, the previous two periods, the previous three periods to the previous $n$ periods.

Then, using Simple Moving Average to analyze the tidal water level data of Su'ao tidal station from January 2004 to September 2021. When the period of the moving average is one year, the moving average of the water level at the Su'ao tidal station and the trend line can be obtained as shown in Fig. 2. From January 2004 to September 2021, the average sea level rise rate of Su'ao tidal station was 2.78 mm/yr, and the rising height was about 0.049 m.

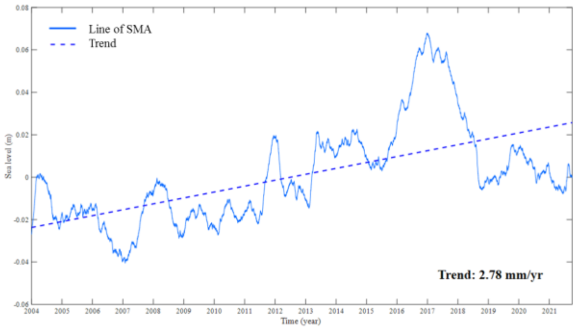


Fig. 2. Line of SMA and trend at Su'ao tidal station.

### B. Hilbert-Huang Transform

Hilbert-Huang Transform (HHT) is an algorithm composed of Empirical Mode Decomposition (EMD) and Hilbert Transform (HT). Huang *et al*. [11] decomposed the signal into multiple Intrinsic Mode Functions (IMFs), and these IMF components are not all complete and symmetrical sine waves. Because the period and amplitude are not fixed, meaningful instantaneous frequency and instantaneous amplitude can be obtained directly using HT. The EMD of HHT is the process of decomposing the signal into multiple IMF components. This process of decomposing into multiple IMF components requires multiple iterations before each IMF can be obtained. The process of decomposing EMD into multiple IMF components is shown in Fig. 3.

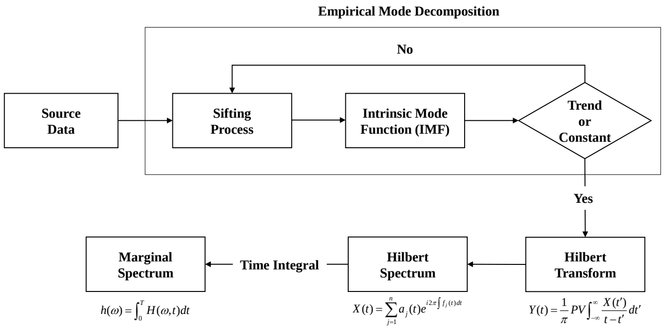


Fig. 3. HHT calculation flow chart.

The calculation process of HHT is to find all local maxima and local minima after inputting the original signal. Then, all local maxima and local minima are subjected to curve fitting, and then cubic spline interpolation is used. After using the cubic spline interpolation, it can get the upper and lower envelopes. Then, after averaging the upper and lower envelopes, the mean envelope A can be obtained. After obtaining the mean envelope $m_1(t)$, subtract the mean envelope $m_1(t)$ from the value of the original signal to obtain the first component $h_1(t)$, as shown in Eq. (15):

$$h_1(t) = s(t) - m_1(t) \tag{15}$$

After finding the first component $h_1(t)$, check whether there is a sum of the number of local maxima and local minima, and whether the number of zero-crossings is equal, or the difference is 1. Also at any point in time, the condition must be met that the average of the upper and lower envelopes approaches zero. If the above conditions are not met, you must continue to filter, use $h_1(t)$ as the original signal, and repeat the steps of cubic spline interpolation and mean envelope, as shown in Eq. (16):

$$h_2(t) = h_1(t) - m_2(t) \tag{16}$$

Repeat the above actions $k$ times, as shown in Eq. (17), until the condition of the IMF component is met.

$$h_k(t) = h_{k-1}(t) - m_k(t) \tag{17}$$

When $h_k(t)$ meets the conditions of the IMF component, the first IMF component $c_1(t)$ can be obtained, as shown in Eq. (18):

$$c_1(t) = h_k(t) \tag{18}$$

Then subtract $c_1(t)$ from the original signal $s(t)$ to obtain the residual signal $r_1(t)$, as shown in Eq. (19):

$$r_1(t) = s(t) - c_1(t) \tag{19}$$

Next, take $r_1(t)$ as a new original signal, repeat the above calculation process, and obtain new residual signals $r_2(t)$, $r_3(t)$, ..., $r_n(t)$ in sequence, as shown in Eqs. (20)–(22):

$$r_2(t) = r_1(t) - c_2(t) \tag{20}$$

$$r_3(t) = r_2(t) - c_3(t) \tag{21}$$

$$r_n(t) = r_{n-1}(t) - c_n(t) \tag{22}$$

When $r_n(t)$ becomes a constant or monotonic function and can no longer be decomposed into IMF components, the decomposition process of EMD is completed. The final original signal can be represented by the sum of all IMF components and the average trend component $r_n(t)$, as in Eq. (23):

$$s(t) = \sum_{k=1}^{n} c_k(t) + r_n(t) \tag{23}$$

After the original signal goes through EMD, each IMF component can be obtained, and then the Hilbert Spectrum can be obtained by HT, as shown in Eq. (24):

$$X(t) = a_j(t)e^{i2\pi\int f_j(t)dt} \tag{24}$$

If the time boundary is defined, the Marginal Spectrum can be obtained, such as in Eq. (25):

$$h(\omega) = \int_0^T H(\omega,t)dt \tag{25}$$

However, simple EMD will have mode mixing. Mode mixing is a phenomenon in which different scales (different amplitudes) can be observed in a certain IMF component, or the same scale (same amplitude) occurs in different IMF components. Mode mixing will cause the IMF components to lose their physical meaning, which will affect the results of subsequent analysis. Therefore, Wu & Huang (2009) [12] improved EMD and concluded Ensemble Empirical Mode Decomposition (EEMD), adding white noise to the signal to be decomposed. The relationship between random number timing and signal is in Eq. (26):

$$\varepsilon_n = \frac{\varepsilon}{\sqrt{N}} \tag{26}$$

where $N$ is the total number of times, $\varepsilon$ is the amplitude of the random number added to the original signal, and $\varepsilon_n$ is the standard deviation of the final error. Since white noise is a signal of small amplitude, it is a random signal, and its energy is uniform. Wu and Huang [12] suggested to use 0.2 times the standard deviation of the original data as the noise amplitude. Because the added white noise can be eliminated at the end, the original signal will not be disturbed.

This study applied the HHT treatment water level data developed by Huang *et al*. [11] and Shen *et al*. [13]. By analyzing the data of the Su'ao tidal station from January 2004 to September 2021, after EMD calculation, the water level variation trend as shown in Fig. 4 and the energy distribution diagram of each IMF components in Fig. 5 can be obtained. From Fig. 5, it can be obtained that the main component of Su'ao tidal station is IMF 1. Therefore, the result of IMF 1 is then converted from the time domain to the frequency domain using Fast Fourier Transform (FFT) as shown in Fig. 6. The frequency is 1.9323 times/day, the period is 0.5175 days. According to the analysis data, the sea level rise of Su'ao tidal station is about 0.054m.

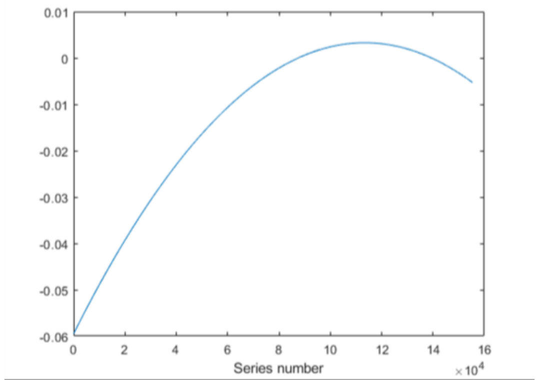


Fig. 4. Trend diagram (EMD) of Su'ao tidal station.

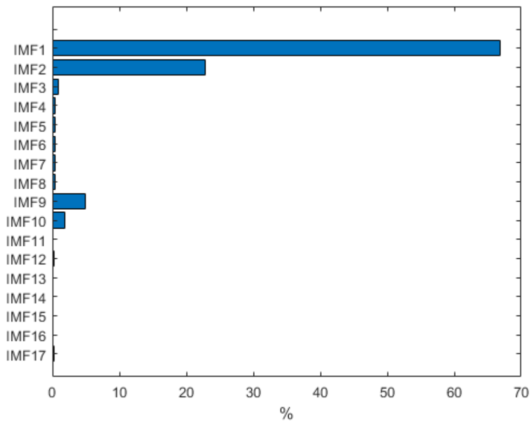


Fig. 5. IMF Energy Distribution Diagram (EMD) of Su'ao tidal station.

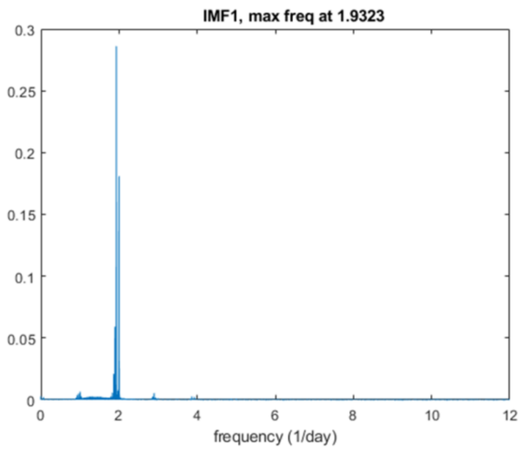


Fig. 6. Spectrogram of IMF 1 component (EMD) of Su'ao tidal station.

Using the EEMD developed by Wu and Huang [12] to analyze the water level data from January 2004 to September 2021, the results in Figs 7-8 can be obtained. The standard deviation of the original data of Su'ao tidal station from January 2004 to September 2021 is 0.4, the amplitude of white noise is 0.08, and the overall frequency is 100. After calculation, the trend of water level change is shown in Fig. 7, and the energy distribution of the IMF components are shown in Fig. 8. It can be known from the energy distribution of IMFs in Fig. 8 that the main component of Su'ao tidal station is IMF 1. Converting IMF 1 from time domain to frequency domain as shown in Fig. 9 by FFT, the frequency is 1.9323 times/day and the period is 0.5175 days. From the results of analyzing the data of Su'ao tidal station, it can be obtained that the sea level rise of Su'ao tidal station is about 0.073m.

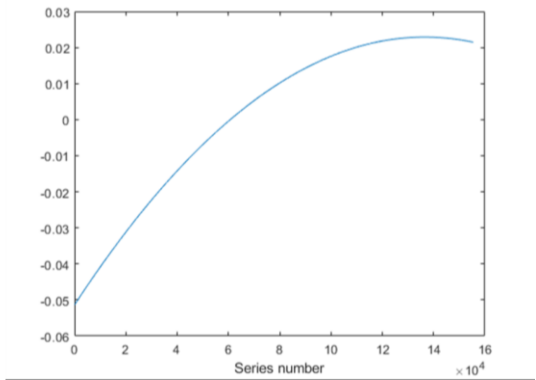


Fig. 7. Trend diagram (EEMD) of Su'ao tidal station.

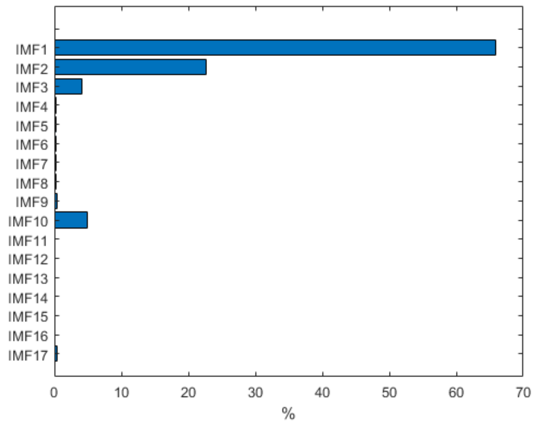


Fig. 8. IMF Energy Distribution Diagram (EEMD) of Su'ao tidal station.

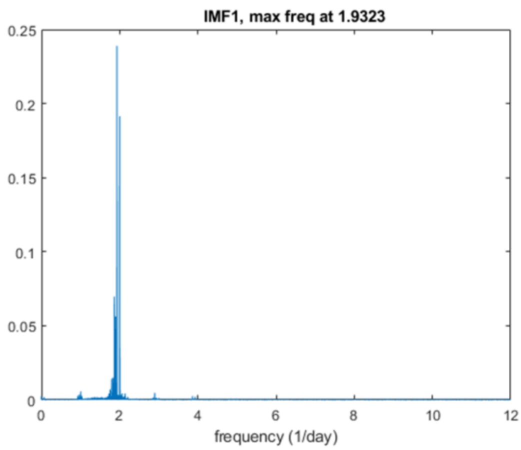


Fig. 9. Spectrogram of IMF 1 component (EEMD) of Su'ao tidal station.

## IV. Conclusion

With the influence of global warming and climate change, the result of the rise of global sea level may raise the storm tide level, which will reduce the functionality of the original coastal protection projects. In order to analyze the long-term changes of sea level in the Yilan Sea area under climate change, this study applied Simple Moving Average (SMA), Empirical Mode Decomposition (EMD) and Ensemble Empirical Mode Decomposition (EEMD) of Hilbert-Huang Transform (HHT), and use these methods to analyze sea level rise. By analyzing the tide level data in the Yilan area from January 2004 to September 2021, using the SMA calculation, it can be obtained that the average sea level rise rate is 2.78 mm/yr, and the rising height is 0.049 m; by EMD calculation, it can be obtained that the average sea level rise rate is 3.04

mm/yr, and the rising height is 0.054 m; and by EEMD calculation, it can be obtained that the average sea level rise rate is 4.11 mm/yr, and the rising height is 0.073 m.

## Conflict of Interest

The authors declare no conflict of interest.

## Author Contributions

H. M. Fang and H. Y. Wang determined the topic and content of the research; P. H. Chang and H. Y. Wang collected data and analyzed it; H. M. Fang and H. Y. Wang did the final synthesis and wrote the paper; all authors had approved the final version.

## References


[1] B. C. Douglas, "Chapter 3 Sea level change in the era of the recording tide gauge," *International Geophysics*, vol. 75, pp. 37–64, 2001.

[2] J. X. Mitrovica, M. E. Tsimplis, J. L. Davis, and G. A. Milne, "Recent mass balance of polar ice sheets inferred from patterns of global sea-level change," *Nature*, vol. 409, pp. 1026–1029, 2001.

[3] J. A. Church, N. J. White, R. Coleman, K. Lambeck, and J.X. Mitrovica, "Estimates of regional distribution of sea level rise over the 1950-2000 period," *Journal of Climate*, vol. 17, pp. 2609–2625, 2004.

[4] J. Church, and N.J. White, "Sea-level rise from the late 19th to the Early 21st Century," *Surveys in Geophysics*, vol. 32, pp. 585-602, 2011.

[5] C. K. Shum, and C. Y. Kuo, "Observation and geophysical causes of present-day sea level rise," *Climate Change and Food Security in South Asia*, pp. 85–104, 2011.

[6] D. Chen, M. Rojas, B. H. Samset, K. Cobb, A. Diongue Niang, and P. Edwards, "Framing, context, and methods," *Climate change 2021: The physical science basis. Contribution of Working Group I to the Sixth Assessment Report of the Intergovernmental Panel on Climate Change*, Cambridge University Press, 2021.

[7] M. A. Merrifield, "A shift in western tropical Pacific sea level trends during the 1990s," *Journal of Climate*, vol. 24, No. 15, pp. 4126-4138, 2011.

[8] D. J. Doong, K. T. Tzeng, and I. S. Yang, "Sea level fluctuation at keelung and kaohsiung," in *Proc. the 30th Ocean Engineering Conference in Taiwan*, pp. 625–630, 2008.

[9] C. Y. Kuo, L. C. Lin, W. H. Lan, W. J. Juang, and C. Y. Lee, *Projection of Future Sea Level Changes around Taiwan*, Institute of Transportation, Ministry of Transportation and Communications, 2016.

[10] Taiwan Climate Change Projection Information and Adaptation Knowledge Platform, *Key Findings in Climate Science from IPCC AR6 Report—Taiwan Edition, Ministry of Science and Technology*, Taiwan, 2021.

[11] N. E. Huang, Z. Shen, S. R. Long, M. C. Wu, H. H. Shih, Q. Zheng, N. C. Yen, C. C. Tung, and H. H. Liu, "The empirical mode decomposition and the Hilbert spectrum for nonlinear and non-stationary time series analysis," in *Proc. the Royal Society A*, vol. 454, pp. 903-995, 1998.

[12] Z. Wu, and N. E. Huang, "Ensemble Empirical Mode Decomposition: A Noise Assisted Data Analysis Method," *Advances in Adaptive Data Analysis*, vol. 1, no. 1, pp. 1–41, 2009.

[13] N. E. Huang, Z. Shen, and S. R. Long, "A new view of water waves—The Hilbert spectrum," *Annual Review of Fluid Mechanics*, vol. 31, pp. 417–457, 1999.